Instant strong and responsive underwater adhesion manifested by bioinspired supramolecular polymeric adhesives

Wu, Jiang; Lei, Handan; Fang, Xinzi; Wang, Bao; Yang, Guang; O'Reilly, Rachel; Wang, Zhongkai; Hua, Zan; Liu, Guangming

DOI:
10.1021/acs.macromol.1c02361

Document Version
Peer reviewed version

Citation for published version (Harvard):
Wu, J, Lei, H, Fang, X, Wang, B, Yang, G, O'Reilly, R, Wang, Z, Hua, Z & Liu, G 2022, 'Instant strong and responsive underwater adhesion manifested by bioinspired supramolecular polymeric adhesives', *Macromolecules*, vol. 55, no. 6, pp. 2003-2013. https://doi.org/10.1021/acs.macromol.1c02361

Instant Strong and Responsive Underwater Adhesion Manifested by Bioinspired Supramolecular Polymeric Adhesives

Jiang Wu,[a] Handan Lei,[a] Xinzi Fang,[a] Bao Wang,[a] Guang Yang,[a] Rachel K. O'Reilly,[c] Zhongkai Wang[a], Zan Hua*[a] and Guangming Liu*[b]*

[a]Biomass Molecular Engineering Center and Department of Materials Science and Engineering, Anhui Agricultural University, Hefei, Anhui 230036, China

[b]Department of Chemical Physics, Key Laboratory of Surface and Interface Chemistry and Energy Catalysis of Anhui Higher Education Institutes, University of Science and Technology of China, Hefei, Anhui 230026, China

[c]School of Chemistry, University of Birmingham, Edgbaston, Birmingham B15 2TT, UK

KEYWORDS: Supramolecular adhesives, Bioinspired materials, Nucleobases, Supramolecular chemistry, Biobased polymers

Entry for the Table of Contents

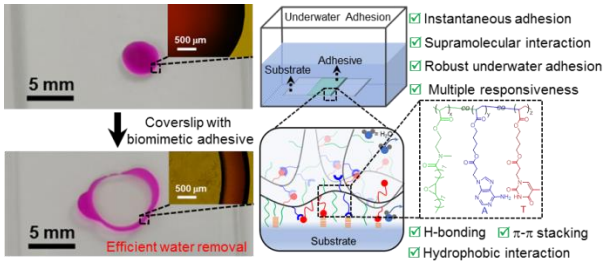

ABSTRACT: Instant strong and responsive underwater adhesion is significant for many biomedical, industrial, and household applications. However, underwater adhesives simultaneously possessing these advantages are challenging to fabricate, because strong and responsive adhesions are usually opposing properties. Herein, we have prepared bioinspired supramolecular polymeric adhesives containing complementary nucleobase moieties in nucleic acids, and have demonstrated an instantaneous underwater adhesion with an adhesion strength reaching as high as 1.5 MPa. Strong underwater adhesion is attributed to the high capability of the adhesives to substantially remove the interfacial water, which can be further modulated by temperature, light, and pH. The excellent underwater adhesion performances have been achieved on various substrates and under distinct aqueous conditions, showcasing the wide applications of the bioinspired nucleobase-containing adhesives developed here. This work opens up a new opportunity for fabricating underwater adhesives for diverse applications with the combined advantages of instant strong and responsive adhesion.

INTRODUCTION

Underwater adhesion is of high significance for many applications such as underwater repair,[1] wound dressing,[2-4] and implantable biomedical devices,[5-7] to name just a few.[8-10] In comparison to the adhesion in a dry environment, efficient underwater adhesion is much more challenging, considering that the presence of a water layer prevents the intimate contact between adherends and adhesives. Underwater adhesives based on hydrogels,[11-17] polymeric films,[18, 19] and supramolecular monomers[1, 20] have been explored. To improve upon the weak underwater adhesion often achieved due to the water layer, two main strategies are often applied to address this issue. The first strategy uses hydrogels, which are able to absorb the water layer on their surface achieving efficient interfacial binding through covalent bonding and supramolecular interactions.[5, 8] Given that the major constituent of hydrogels is water, the efficiency of binding between the substrate and the adhesive is low with the adhesion strength of often less than 200 kPa.[16, 21] The other strategy involves the selection of hydrophobic moieties for incorporation into adhesives, as these can be employed to expel the water layer on the adherend's surface.[2, 12, 17] Perhaps the most widely used chemistry to date is catechol chemistry which has been inspired by marine organisms such as mussels and tubeworms.[22, 23] Through a combination of catechol groups and hydrophobic moieties such as phenyl groups, researchers have been able to achieve robust underwater adhesives as high as 3.0 MPa for aluminum.[24] However, the easy oxidation of catechol in the adhesives also limits the application scope by diminishing both the cohesive and adhesive properties.

It is highly desirable to achieve an instant strong and responsive underwater adhesion, as this would enable highly efficient adhesion and removal of adhesives immediately when

needed.[25, 26] However, strong and responsive adhesions are opposing and appear to be incompatible properties, because a strong adhesion usually relies on robust and irreversible covalent interactions and a long curing time over several hours.[1, 24, 27] In contrast to covalent bonding, supramolecular interactions, including H-bonding, π-π stacking, and hydrophobic interactions, endow adhesives with outstanding stimuli-responsiveness. Therefore, it is highly feasible to achieve strong and responsive underwater adhesion by combining multiple supramolecular interactions in adhesives. Nucleic acids in nature provide us with excellent models for robust interactions that are responsive by simply utilizing supramolecular interactions such as H-bonding, π-π stacking, and hydrophobic interactions. By taking advantage of the elegant supramolecular interactions between nucleobases, materials chemists have demonstrated the fabrication of functional polymeric materials, including supramolecular aggregates,[28-34] nanostructures with programmable morphological transformation,[35-38] self-healing materials,[39] and polymeric adhesives.[16, 40-44] Nucleobase-containing adhesives have recently emerged as a new class of strong adhesive materials which can operate under ambient conditions, utilizing multiple supramolecular interactions to achieve adhesion. Importantly, nucleobase-containing polymeric adhesives have robust and also dynamic properties due to the characteristics of multiple supramolecular interactions, which is essential to achieve strong and responsive underwater adhesion.

Our recent work employed nucleobase-containing copolymers as adhesives and the polymers with individual nucleobases have moderate adhesive properties. The adhesion strength of nucleobase-containing adhesives can be further enhanced through mixing the copolymers with complementary nucleobases. The supramolecular mixtures can effectively form the intermolecular H-bonding, giving rise to the improvement of adhesion strength. This inspired us to develop and

fabricate stronger adhesives through elegantly designing the molecular architectures and network structures. Herein, a new type of instant strong and responsive underwater polymeric adhesives was successfully fabricated by combining bioinspired supramolecular interactions between complementary nucleobases with hydrophobic interactions imparted by long alkyl chains derived from renewable plant oils (Figure 1). The current system utilizes the ternary copolymerization of plant oil-based monomer and complementary nucleobase-containing monomers to produce adhesives with both inter- and intramolecular H-bonding moieties. The new copolymers can form a more homogeneous polymer network structure for better energy dissipation through the disassociation and reformation of inter- and intramolecular H-bonding interaction. These bioinspired hydrophobic supramolecular adhesives are able to efficiently remove the interfacial water layer, achieving an immediately strong underwater adhesion. Multiple supramolecular interactions—rather than covalent bonding—impart strong cohesive and adhesive capacity to the adhesives within 10 s, avoiding a long curing time. The properties of supramolecular adhesives can be further modulated through the application of external stimuli such as temperature or UV irradiation, enabling responsive underwater adhesion behavior with an adhesion strength as high as 1.5 MPa. Underwater strong adhesion based on supramolecular interactions imbues the adhesives with quick adhesion without a long time curing and good stimuli-responsiveness. The hydrophobic nucleobase-containing adhesives based on supramolecular interactions result in an efficient adhesion on 7 distinct substrates and under various underwater environments including seawater, different pHs, and in the presence of organic solvents. It is envisaged that the instant strong and responsive supramolecular adhesives would find many important applications for urgent underwater adhesion and repair.

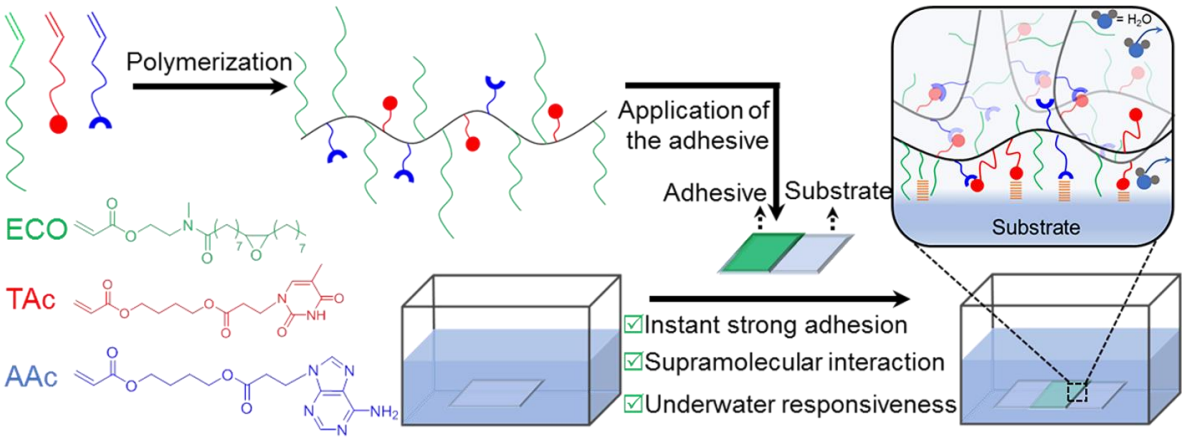

Figure 1. Schematic illustration of the fabrication of underwater supramolecular adhesives with instant strong and responsive adhesion.

RESULTS AND DISCUSSION

Synthesis and characterization of bioinspired hydrophobic nucleobase-containing copolymers

In order to prepare adhesives with high hydrophobicity and strong inter- and intramolecular interactions, the preparation and ternary copolymerization of the hydrophobic epoxidized camellia oil monomer (ECO), 4-((3-(adenine-9-yl)propanoyl)oxy)butyl acrylate (AAc) and 4-((3-(thymin-1-yl)propanoyl)oxy)butyl acrylate (TAc) with complementary H-bonding moieties was carried out according to the literature with slight modifications (Schemes S1-S2 and Figures S1-S3).[43, 45, 46] A series of copolymers $P_{x\text{-}y\text{-}z}$ were obtained *via* conventional free radical polymerization with AIBN as the initiator in DMF solution at 75 °C, in which x, y, and z represent the molar percent of ECO, AAc, and TAc, respectively.

The representative ^{1}H NMR spectrum of the copolymer $P_{70\text{-}15\text{-}15}$ has signals at 12.56, 6.74 and 0.86 ppm, attributing to the proton connected to N3 in thymine, NH_2 in adenine and CH_3 at the chain end in ECO, respectively (Figure 2a and Figure S3). Interestingly, the supramolecular H-bonding interaction between adenine and thymine in the copolymers

gives rise to a gradual low field shift of the peaks for the protons involving the complementary H-bonding interaction (Figure 2b). This result illustrates that the complementary H-bonding interaction was reinforced with higher nucleobase contents in the copolymers. Further study shows that the chemical shifts of protons (6.74 and 12.56 ppm) in nucleobase moieties of $P_{70\text{-}15\text{-}15}$ at various concentrations (5, 10 and 20 mg mL^{-1}) are almost identical (Figure S4). This suggests the change of the chemical shifts of copolymers mainly arises from the intramolecular H-bonding interaction, owing to the relative low concentration (*ca.* 10 mg mL^{-1}) for NMR measurements. SEC traces of all the attained copolymers show relatively broad molecular weight distributions ($Đ$ = ~3.00), which could be attributed to the conventional radical polymerization and multiple H-bonding moieties in the copolymers (Table 1 and Figure S5). Thermal properties of obtained copolymers were characterized by thermogravimetric analysis (TGA) and differential scanning calorimetry (DSC). The copolymers display good thermal stability with the decomposition temperatures over 280 °C (Figure 2c and Table 1). The DSC curves of all copolymers show a single glass transition temperature (T_g) from -19.0 °C for $P_{90\text{-}5\text{-}5}$ to 13.4 °C for $P_{30\text{-}35\text{-}35}$, suggesting a random copolymerization of these monomers (Figure 2d). A positive deviation from the classical Fox equation was observed for the copolymers (Figure S6). These results were attributed to the strong interaction between nucleobase moieties including π-π stacking and complementary H-bonding, which is consistent with the previous publications.[42-43] In addition, all obtained copolymers have similar M_ws from 48.5 to 96.3 kDa (Table 1 and Figure S5), playing a negligible effect on the T_gs of copolymers. Therefore, considering that the nucleobase-containing monomers contain rigid purine and pyrimidine groups and tend to form

complementary H-bonding, the resulting copolymers incorporating more nucleobase moieties are anticipated to have a higher T_g due to the decrease in chain mobility.

Table 1. Molecular characterization data of P(ECO-*co*-AAc-*co*-TAc) copolymers with various nucleobase contents.

Polymer	Structure	M_w[a] (kDa)	$Đ_M$[a]	T_g[b] (°C)	T_d[c] (°C)
$P_{30\text{-}35\text{-}35}$	P($ECO_{0.3}$-*co*-$AAc_{0.35}$-*co*-$TAc_{0.35}$)	90.5	2.78	13.4	281.3
$P_{40\text{-}30\text{-}30}$	P($ECO_{0.4}$-*co*-$AAc_{0.3}$-*co*-$TAc_{0.3}$)	96.3	2.86	10.7	286.2
$P_{50\text{-}25\text{-}25}$	P($ECO_{0.5}$-*co*-$AAc_{0.25}$-*co*-$TAc_{0.25}$)	76.5	3.21	3.0	289.3
$P_{60\text{-}20\text{-}20}$	P($ECO_{0.6}$-*co*-$AAc_{0.2}$-*co*-$TAc_{0.2}$)	64.3	3.06	-4.3	293.8
$P_{70\text{-}15\text{-}15}$	P($ECO_{0.7}$-*co*-$AAc_{0.15}$-*co*-$TAc_{0.15}$)	68.9	3.19	-7.5	313.7
$P_{80\text{-}10\text{-}10}$	P($ECO_{0.8}$-*co*-$AAc_{0.1}$-*co*-$TAc_{0.1}$)	51.6	3.00	-9.1	320.8
$P_{90\text{-}5\text{-}5}$	P($ECO_{0.9}$-*co*-$AAc_{0.05}$-*co*-$TAc_{0.05}$)	48.5	3.11	-19.0	323.9

[a]Determined by DMF SEC with poly(methyl methacrylate) (PMMA) standards. [b]Measured by DSC from the second scan from −70 °C to 70 °C at a rate of 10 °C min^{-1}. [c]Measured by TGA from 40 to 700 °C at a rate of 10 °C min^{-1}, the values represent the 5% degradation point of the copolymers.

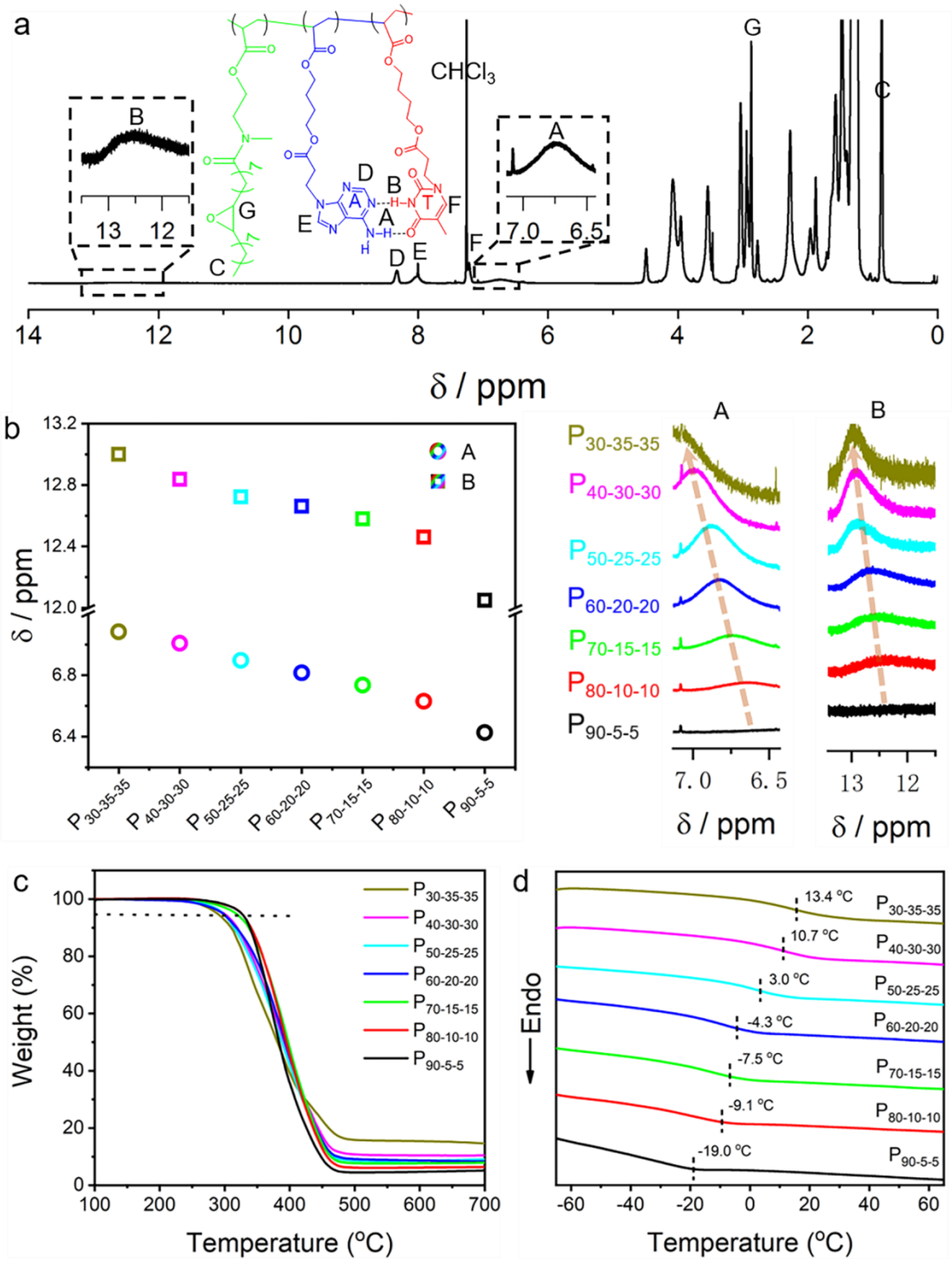

Figure 2. Molecular characterization and thermal analyses of nucleobase-containing copolymers. (a) Representative ^{1}H NMR spectrum of the P(ECO$_{0.7}$-*co*-AAc$_{0.15}$-*co*-TAc$_{0.15}$) (P$_{70\text{-}15\text{-}15}$) copolymer in $CDCl_3$. (b) Chemical shifts of protons from adenine and thymine involving the complementary H-bonding interaction change from P$_{90\text{-}5\text{-}5}$ to P$_{30\text{-}35\text{-}35}$. (c) TGA curves and (d) DSC curves of P(ECO-*co*-AAc-*co*-TAc) copolymers with different monomer compositions.

Instant strong underwater adhesion of P(ECO-*co*-AAc-*co*-TAc) copolymers

Nucleobase-containing copolymers P(ECO-*co*-AAc-*co*-TAc)s are expected to have good underwater adhesive properties with the presence of H-bonding interactions, π-π stacking, and hydrophobic interactions. Firstly, a glass slide was coated with polymer solution (50 mg mL^{-1} in CH_2Cl_2) and dried, then it was immersed in water and bonded with another clean glass slide underwater for 10 s with 20 N loading. Indeed, the copolymers displayed outstanding underwater adhesive strengths on measuring the shear strength of two copolymer-bonded glass slides with a contact area of 0.25 cm^2 at 25 °C (Figure 3a). The underwater adhesive strength at 25 °C increases from 190 ± 12 kPa for $P_{90\text{-}5\text{-}5}$ to 830 ± 72 kPa for $P_{70\text{-}15\text{-}15}$. Since cohesive failures were observed for all these copolymers, the increase of adhesive strength should be attributed to the stronger intermolecular H-bonding interaction with higher nucleobase contents. Further increase of nucleobase monomers results in a decrease in adhesion strength to 160 ± 40 kPa for $P_{50\text{-}25\text{-}25}$. The drop in adhesion strength of copolymers with more nucleobase moieties could be caused by the relatively high glass transition temperatures. This property makes the adhesive difficult to wet the substrate, leading to poor adhesive properties. As expected, $P_{40\text{-}30\text{-}30}$ and $P_{30\text{-}35\text{-}35}$ copolymers with nucleobase monomers over 50 mol% are not capable of forming effective bonding between two glass slides at 25 °C due to their higher T_gs. In order to explore the durability of underwater adhesion, glass plates bonded by $P_{70\text{-}15\text{-}15}$ were immersed into water at 25 °C for different time and the adhesion strengths were further measured. The adhesion strength of $P_{70\text{-}15\text{-}15}$ can sustain over 800 kPa after immersing in water for over 5 days with a slow drop afterwards, demonstrating strong and long-lasting underwater adhesion (Figure S7).

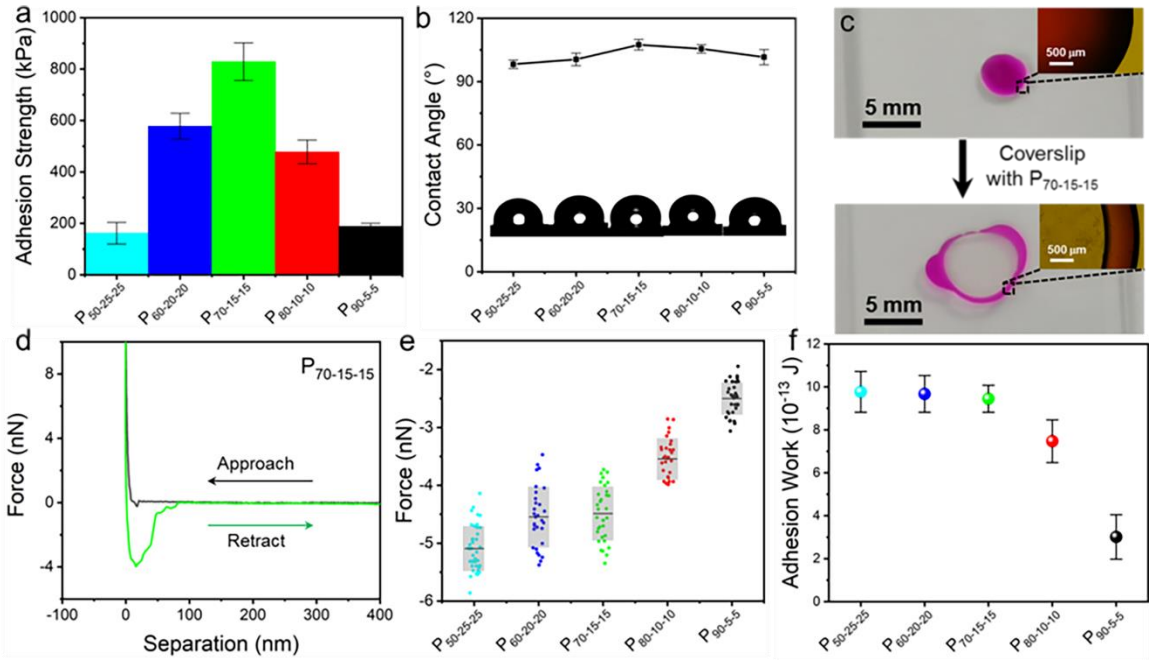

Figure 3. Characterization of the underwater adhesion of P(ECO-*co*-AAc-*co*-TAc) copolymers. (a) Underwater adhesive strengths of copolymers from $P_{90\text{-}5\text{-}5}$ to $P_{50\text{-}25\text{-}25}$ on bonding two glass slides with a contact area of 0.25 cm^2 at 25 °C. (b) Water contact angles (WCAs) of glass slides coated with nucleobase-containing copolymers from $P_{90\text{-}5\text{-}5}$ to $P_{50\text{-}25\text{-}25}$. (c) Photographs and fluorescent images of a water droplet (with rhodamine B) without and with the coverslip coating with the adhesive $P_{70\text{-}15\text{-}15}$, indicating the efficient removal of the interfacial water layer by $P_{70\text{-}15\text{-}15}$. (d) A representative underwater AFM approaching-retracting curve for $P_{70\text{-}15\text{-}15}$. (e) Underwater adhesive force and (f) adhesion work of bioinspired hydrophobic nucleobase-containing adhesives from $P_{90\text{-}5\text{-}5}$ to $P_{50\text{-}25\text{-}25}$ measured by AFM with a silicon tip and a SiO_2 probe of 3.5 μm in diameter, respectively. Box plots show the mean values (the black line) and error bars (the grey box) over 30 measurements.

Removal of the water layer in the interface using hydrophobic adhesives with multiple H-bonding moieties could be a highly promising and feasible way to achieve a strong underwater adhesion with more adhesive sites. Intriguingly, the underwater adhesive strength of hydrophobic nucleobase-containing copolymers is dramatically stronger than that of hydrogels, polymeric films and polypeptides (Figure S8). The presence of a water layer and the lack of bonding sites are two unavoidable factors impeding the formation of a strong underwater adhesion. To reveal how strong underwater bonding is achieved with

the nucleobase-containing copolymers, a series of investigations were carried out. Firstly, the spin-coating films of these copolymers from $P_{90\text{-}5\text{-}5}$ to $P_{50\text{-}25\text{-}25}$ all manifest high hydrophobicity with water contact angles (WCAs) of about 100° (Figure 3b), indicating that the long alkyl chains (C18 structure) in ECO imbue the copolymers with excellent hydrophobicity even when the copolymer is composed of nucleobase-containing monomers at 50 mol%. In order to understand why the water contact angles slightly change with the copolymer composition, two control homopolymers PTAc and PAAc were successfully synthesized through free radical polymerization, which was confirmed by using ^{1}H NMR spectroscopy (Figure S9a). The homopolymers were dissolved in DMSO and spin-coated on the silicon wafer followed by drying in vacuo at 70 °C overnight. Water contact angles of both PTAc and PAAc were about 75°, which is not very hydrophilic (Fig. S9b). Therefore, the introduction of TAc and AAc would not change the hydrophobicity of the copolymer significantly. In addition, the efficient bonding can be achieved with over 2 N loading after bonding for over 10 s, showing the easy applicability underwater for the current adhesives (Figure S10).

Further, an aqueous solution with rhodamine B was dropped on a clean glass slide, which was immediately covered with a coverslip containing the adhesive $P_{70\text{-}15\text{-}15}$ (Figure 3c). This experiment shows that the hydrophobic adhesive $P_{70\text{-}15\text{-}15}$ can immediately remove the water droplet with a light pressure. The presence of the colorless area indicates that the adhesive is capable of efficiently removing the interfacial water layer. Meanwhile, no detectable fluorescence was observed for the area covered with the adhesive, suggesting that the water layer was fully removed from the surface (Figure 3c). These properties are of great significance for the instantly strong adhesive performance in the presence of water.

We used AFM to investigate the underwater interfacial force of our copolymers at the nanoscale. The AFM tip (Bruker, Silicon tip on nitride lever) was initially brought to the underwater adhesive coating surface, then retracted (at tip-substrate separation distance, D = 0). The maximum force applied to separate the tip from the surface was determined as the adhesion force. The representative approach-retraction curve of the adhesive $P_{70\text{-}15\text{-}15}$ is shown in Figure 3d. The adhesive force was on the order of several nanonewtons and the debonding distance was over one hundred nanometers, demonstrating efficient underwater adhesion. In contrast, $P_{80\text{-}10\text{-}10}$ and $P_{90\text{-}5\text{-}5}$, with lower nucleobase content, resulted in lower adhesion forces and shorter debonding distances (Figure 3e and Figure S11). In order to quantitatively compare the work of adhesion for different copolymers, an AFM probe with colloidal SiO_2 particles of 3.5 μm in diameter and nominal spring constant of ~0.2 N m^{-1} were used to measure the underwater adhesion strength of copolymers based on JKR type measurements. The adhesion work (W) was calculated according to the equation $W = -\int F \mathrm{d}D$, where the force first became attractive ($F < 0$) and then upon retraction to a large distance the force was 0. The quantified comparison of adhesion work between different copolymers shows an obvious increase in adhesion from $(3.01 \pm 1.04) \times 10^{-13}$ J for $P_{90\text{-}5\text{-}5}$ to $(9.45 \pm 0.63) \times 10^{-13}$ J for $P_{70\text{-}15\text{-}15}$ (Figure 3f), which is consistent with the macroscopic adhesion tests (Figure 3a). No obvious change of nanoscopic adhesion forces and adhesion work was observed when further increasing the nucleobase content, which may be attributable to a saturation of interfacial binding sites at high nucleobase contents.

Thermo-responsive underwater adhesion of bioinspired nucleobase-containing copolymers

Responsive adhesive materials are important in practical applications, not only for immediately repositioning misplaced adhesives but also for removing used adhesives after applications. However, instant strong and responsive underwater adhesions are challenging properties to achieve together, since strong adhesion is often dependent on strong/covalent and non-responsive bonding. The hydrophobic nucleobase-containing adhesives enable us to fabricate instant strong underwater adhesion with a substrate through multiple supramolecular bonding. A stronger adhesion was observed at lower temperatures for all $P_{90\text{-}5\text{-}5}$, $P_{80\text{-}10\text{-}10}$, $P_{70\text{-}15\text{-}15}$ and $P_{60\text{-}20\text{-}20}$ (Figure 4a). For example, the adhesion strength increases from 190 ± 50 kPa at 40 °C, to 830 ± 72 kPa at 25 °C, and further up to 1510 ± 44 kPa at 10 °C for $P_{70\text{-}15\text{-}15}$, showing about 8.0 times increase in adhesion strength with decreasing temperature from 40 to 10 °C. Remarkably, the adhesion strength of $P_{70\text{-}15\text{-}15}$ after immersing into water at 10 °C for 14 days is still as high as 1.36 MPa, which is close to the initial adhesion strength of 1.50 MPa (Figure S12). Meanwhile, all the copolymers from $P_{90\text{-}5\text{-}5}$ to $P_{50\text{-}25\text{-}25}$ (300 mg) were soaked in water (20 mL) for 14 days and the water was freeze-dried to obtain the mass of dissolved copolymers. No discernible copolymers were observed in the water layer, showing good water resistance (Figure S13). These results illustrate the durability of the adhesive underwater. Similar thermo-responsive changes of adhesive properties were also observed for $P_{90\text{-}5\text{-}5}$, $P_{80\text{-}10\text{-}10}$ and $P_{60\text{-}20\text{-}20}$. In contrast, a marked decrease in adhesion strength was observed for $P_{50\text{-}25\text{-}25}$ from 40 to 10 °C, which might be caused by the different interfacial wetting behavior. These nucleobase-containing adhesives without any additives represent a new type of immediately robust underwater adhesives with interesting thermo-tunable properties.

To reveal the thermo-responsive behavior of these adhesives, frequency sweep rheological analyses were conducted from 0.07 to 188 rad s^{-1} at 25 and 40 °C for all P(ECO-*co*-AAc-*co*-TAc) copolymers (Figure 4b and Figures S14-S16). A viscoelastic window can be obtained by employing the shear storage modulus (G') and the shear loss modulus (G'') at frequencies consistent with adhesive bonding (10^{-1} rad s^{-1}) and debonding (100 rad s^{-1}) for pressure sensitive adhesives (PSAs).[47-49] For the copolymers with nucleobase contents less than 40 mol%, the shear storage modulus (G') is always less than shear loss modulus (G'') at different frequencies, thus they are viscous polymers. Meanwhile, they have G' values at the bonding frequency (10^{-1} rad s^{-1}) below the Dahlquist criterion ($G' \leq 3 \times 10^5$ Pa), facilitating the efficient substrate wetting and enabling their use as effective PSAs. An obvious decrease of both moduli was observed when increasing the temperature to 40 °C, suggesting the weakening of intermolecular supramolecular interactions at the elevated temperature.

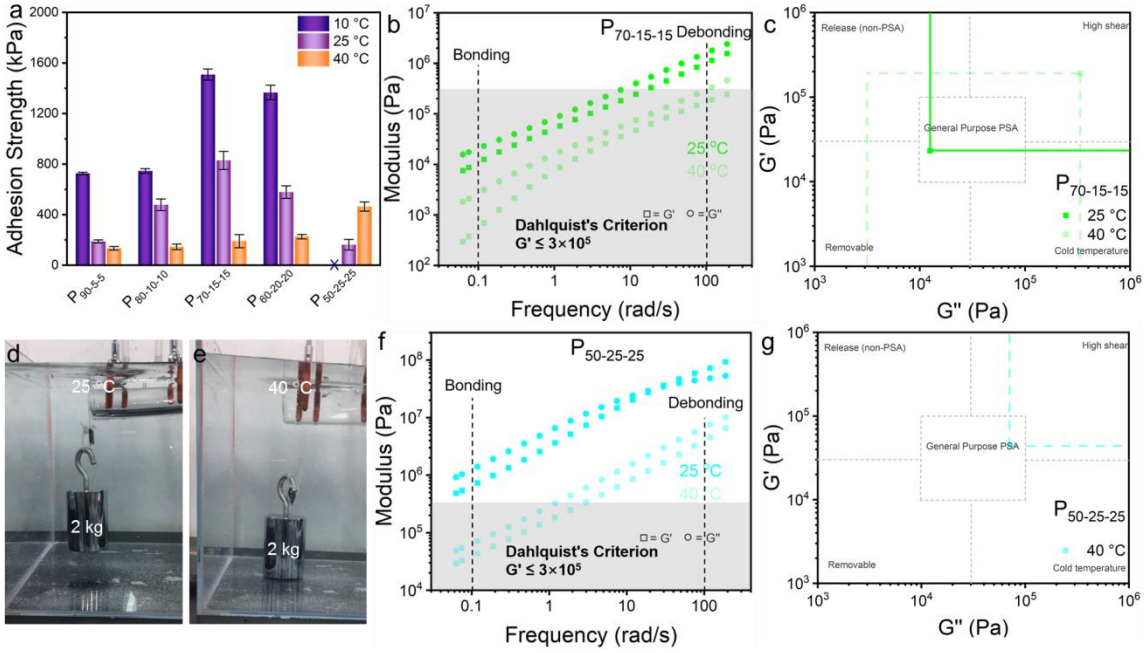

Figure 4. Characterization of underwater thermo-responsive adhesive properties of P(ECO-*co*-AAc-*co*-TAc) copolymers. (a) Underwater adhesion strength of P(ECO-*co*-

AAc-*co*-TAc) copolymers from $P_{90\text{-}5\text{-}5}$ to $P_{50\text{-}25\text{-}25}$ at 10, 25 and 40 °C. Frequency sweep rheological analyses of (b) $P_{70\text{-}15\text{-}15}$ and (f) $P_{50\text{-}25\text{-}25}$ from 0.07 to 188 rad s^{-1} at 25 and 40 °C. Viscoelastic windows for (c) $P_{70\text{-}15\text{-}15}$ and (g) $P_{50\text{-}25\text{-}25}$ copolymers obtained from the bonding (ω = 0.1 rad s^{-1}) and debonding (ω = 100 rad s^{-1}) frequencies at 25 and 40 °C. The photographs taken from Movie S1 (Supporting information) show the thermo-responsive adhesive behaviors of $P_{70\text{-}15\text{-}15}$ at (d) 25 °C and (e) 40 °C.

The properties of nucleobase-containing adhesives were further analyzed according to the quadrant method, providing a qualitative assessment of the adhesion strength at different temperatures.[47-49] For instance, $P_{70\text{-}15\text{-}15}$ shows a high shear strength at 25 °C, and should thus behave as a general purpose PSA at 40 °C due to the decrease in moduli (Figure 4c). To demonstrate the thermo-responsive adhesive behaviors, a 2 kg weight immersed into water was connected to a glass slide bonded to a temperature-controlled chamber (Figure 4d). At 25 °C, the adhesion can be sustained underwater for over 2 h without any obvious change observed. When heating the connected adhesive at 40 °C, the load was dropped within 1 min, demonstrating the fast thermo-responsive adhesive behavior of the polymer (Figure 4e and Movie S1). In contrast, the copolymer $P_{50\text{-}25\text{-}25}$ has a G' value of 7.3 $\times 10^5$ Pa at 10^{-1} rad s^{-1} above the Dahlquist criterion ($G' \leq 3 \times 10^5$ Pa) at 25 °C, preventing the effective wetting of the substrate (Figure 4f and 4g).

Further, tensile tests are used to quantify the hysteresis of the polymers, which is related to the adhesive properties. The copolymers with low nucleobase contents are viscous polymers, which cannot be measured via tensile tests. The copolymer $P_{50\text{-}25\text{-}25}$ with high nucleobase content can be measured via tensile tests to quantify the hysteresis. The maximum stress of 1.12 MPa and strain of 325% were observed for $P_{50\text{-}25\text{-}25}$ via uniaxial tensile testing (Figure S17a). To quantify the energy dissipation capability, cyclic tensile loading measurements of $P_{50\text{-}25\text{-}25}$ without relaxing were conducted for the maximum strain of 250% with 50% increment (Figure S17b). Hysteresis areas for $P_{50\text{-}25\text{-}25}$ were observed to increase with a larger strain, which shows efficient energy

dissipation (Figure S17c). In addition, the copolymer $P_{50\text{-}25\text{-}25}$ has a good damping capacity of over 82% for the strain from 50% to 250% (Figure S17d). These results suggested that the intermolecular H-bonding interaction is able to dissipate the energy through its dissociation and reformation. Overall, $P_{70\text{-}15\text{-}15}$ has better adhesion properties than others, which will be further investigated and explored for its potential applicability.

Tunable underwater adhesion through UV crosslinking of thymine

Efficient crosslinking of nucleobases can be successfully achieved through a photodimerization of pyrimidines under UV irradiation with a wavelength at 302 nm.[50-52] As cohesive failure was observed for the nucleobase-containing adhesives, we wonder whether the intermolecular interaction within $P_{70\text{-}15\text{-}15}$ can be further enhanced through thymine photodimerization, leading to stronger adhesive properties at room temperature. Two quartz glass sheets were attached with $P_{70\text{-}15\text{-}15}$ and exposed to the UV light for different irradiation periods (Figure 5a). The UV crosslinking process was monitored by using UV–vis spectroscopy. A gradual decrease of UV absorbance at 264 nm was observed during the initial 30 min of irradiation, attributed to the covalent crosslinking of thymine (Figure S18). Further prolonging the irradiation time resulted in a slow decrease in the absorbance at 264 nm. As a result, a significant increase of adhesion strength was observed for $P_{70\text{-}15\text{-}15}$ from 710 ± 150 kPa without irradiation to 1430 ± 120 kPa with 30 min of UV irradiation. No obvious increase of adhesion strength was observed when the irradiation time was further extended beyond 30 mins (Figure 5b).

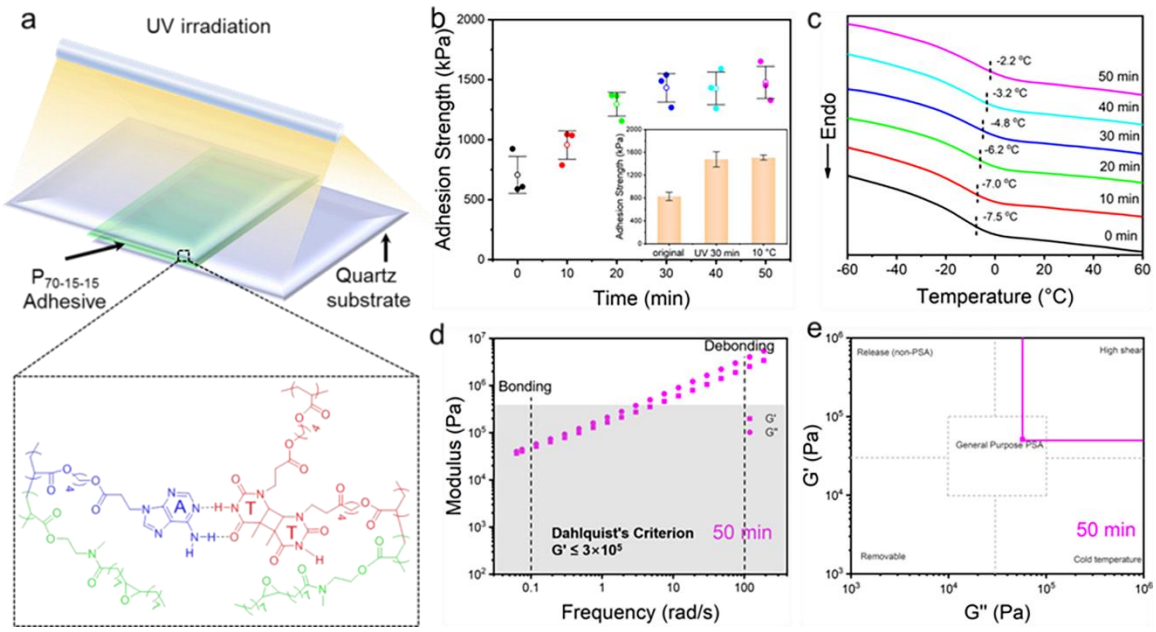

Figure 5. Enhancement in adhesive properties of $P_{70\text{-}15\text{-}15}$ by UV irradiation. (a) Schematic illustration of the UV crosslinking for the adhesive $P_{70\text{-}15\text{-}15}$ and the change of molecular structure upon irradiation. The change in (b) adhesion strength and (c) DSC analyses of $P_{70\text{-}15\text{-}15}$ after different periods of UV irradiation. The inset in (b) shows the efficient enhancement of adhesive properties via UV irradiation or cooling down. (d) The representative frequency sweep rheological analyses of $P_{70\text{-}15\text{-}15}$ after 50 min UV irradiation and (e) its viscoelastic window obtained from the bonding (ω = 0.1 rad s^{-1}) and debonding (ω = 100 rad s^{-1}) frequencies at 25 °C.

The effective covalent crosslinking was further confirmed by determination of the gel content of the adhesive $P_{70\text{-}15\text{-}15}$ formed after UV irradiation (Figure S19 and Table S1). The irradiated adhesives were dissolved with CH_2Cl_2 to extract the soluble copolymer and the weight of the residual gels was compared with the initial weight before irradiation to obtain the gel content. A dramatic increase of gel content was observed during the initial 30 min of irradiation and the rate dropped when the irradiation time was further prolonged (Figure S19). DSC analyses also indicate that covalent crosslinking occurred upon UV irradiation, as reflected by the gradual increase in the glass transition temperature (Figure 5c). As

expected, the thymine photodimerization restricts the mobility of chain segments, yielding a higher T_g value following irradiation.

Rheological analyses show that $G' < G''$ was observed at all frequencies with different irradiation periods, illustrating that the adhesive is a viscous liquid (Figure 5d and Figures S20-S23). Based on the Dahlquist criterion, the result also suggests that adhesives subjected to different irradiation periods can all achieve the efficient wetting of substrates. Furthermore, the shear strength of adhesive gradually becomes stronger with the extension of irradiation time according to the quadrant method (Figure 5e and Figures S20-S23). In contrast, when irradiating the P($ECO_{0.7}$-*co*-$AAc_{0.3}$) without UV crosslinking moieties under the same conditions for 1 h, no obvious change of adhesion strength was observed, indicating the significance of thymine photodimerization for the enhanced adhesive performance (Figure S24). Notably, underwater adhesion strength of P($ECO_{0.7}$-*co*-$AAc_{0.3}$) containing adenine is 548 ± 140 kPa, more than the adhesion strengths of $P_{90\text{-}5\text{-}5}$ and $P_{50\text{-}25\text{-}25}$ with a contact area of 0.25 cm^2 at 25 °C. Considering that the adenine-adenine/thymine-thymine self-association interaction is much weaker than complementary H-bonding between adenine and thymine,[53] the underwater adhesion strength of P($ECO_{0.7}$-*co*-$AAc_{0.3}$) should be weak. However, the additional noncovalent interaction such as π-π stacking is more pronounced for adenine, following purine-purine > purine-pyrimidine > pyrimidine-pyrimidine. As a result, the underwater adhesion strength of $P_{90\text{-}5\text{-}5}$ with low nucleobase content has weaker adhesive properties. Additionally, although $P_{50\text{-}25\text{-}25}$ has a higher nucleobase component of 50 mol%, its high T_g makes the adhesive difficult to wet the substrate, leading to poor adhesive properties. These results illustrate that the synergetic supramolecular and covalent interactions are of great importance to generate a robust and UV-tunable underwater adhesion.

Robust underwater adhesion of bioinspired hydrophobic nucleobase-containing copolymers

Hydrophobic nucleobase-containing adhesives created through strong multiple supramolecular interactions provide a general and facile method to achieve immediately robust underwater adhesion. To showcase the broad applicable scope of these adhesives, their effective interaction with a range of distinct substrates was demonstrated. Underwater adhesive strengths with $P_{70\text{-}15\text{-}15}$ on poly(tetrafluoroethylene) (PTFE), poly(ethylene) (PE), poly(methyl methacrylate) (PMMA), poly(ethylene terephthalate) (PET), glass, iron (Fe) and ceramics can reach 390, 390, 470, 770, 830, 1400 and 1430 kPa, respectively (Figure 6a). For example, two PTFE plates bound by $P_{70\text{-}15\text{-}15}$ with a contact area of 1.0 cm^2 can easily hold a weight of 2 kg (Figure 6b). These results suggest that the hydrophobic supramolecular adhesive has excellent underwater adhesion on a range of substrates. More importantly, the excellent underwater adhesion was formed by the reversible supramolecular interaction rather than covalent bonding, which enables us to execute multiple adhesion-peeling cycles, showing no obvious decay in adhesion strength (Figure S25).

To further expand the applicability of hydrophobic nucleobase-containing adhesives in a range of different aqueous environments, a glass surface coated with $P_{70\text{-}15\text{-}15}$ was adhered with another clean glass surface at different pH conditions (Figure 6c). The adhesion strength was observed to increase from 530 ± 45 kPa at pH = 1.0 to 830 ± 72 kPa at pH = 7.0, which may be as a result of the protonation of the N1 in adenine (pK_a = 3.5) at low pH. The improvement in protonation can trigger the disruption of complementary H-bonding interactions and the increase

in hydrophilicity of adhesives, giving rise to the decrease of adhesion from pH = 7.0 to pH = 1.0. In contrast, the increase of the solution pH from 7.0 to 13.0 leads to loss of adhesion underwater, which can be attributed to the deprotonation of the proton connected to the N3 in the thymine copolymer (p*K*a = 9.9). Therefore, the adhesion strength tends to increase and then decrease with increasing pH value of the aqueous solutions, showing the strongest adhesion at pH = 7.0. Additionally, the hydrophobic strong nucleobase-containing adhesive $P_{70\text{-}15\text{-}15}$ was also compatible with high salt concentrations such as artificial seawater (0.6 M NaCl in water with pH of 6.8), demonstrating an adhesion strength of 900 ± 40 kPa. The underwater adhesive strength is still as high as 800 kPa after exposing in seawater for 7 days (Figure S26). This result indicates that the supramolecular adhesives reported here have the durable underwater adhesive properties underwater, which is essential for the potential applications. The robust hydrophobic nucleobase-containing adhesives show good tolerance to the nature of the exterior aqueous underwater environments.

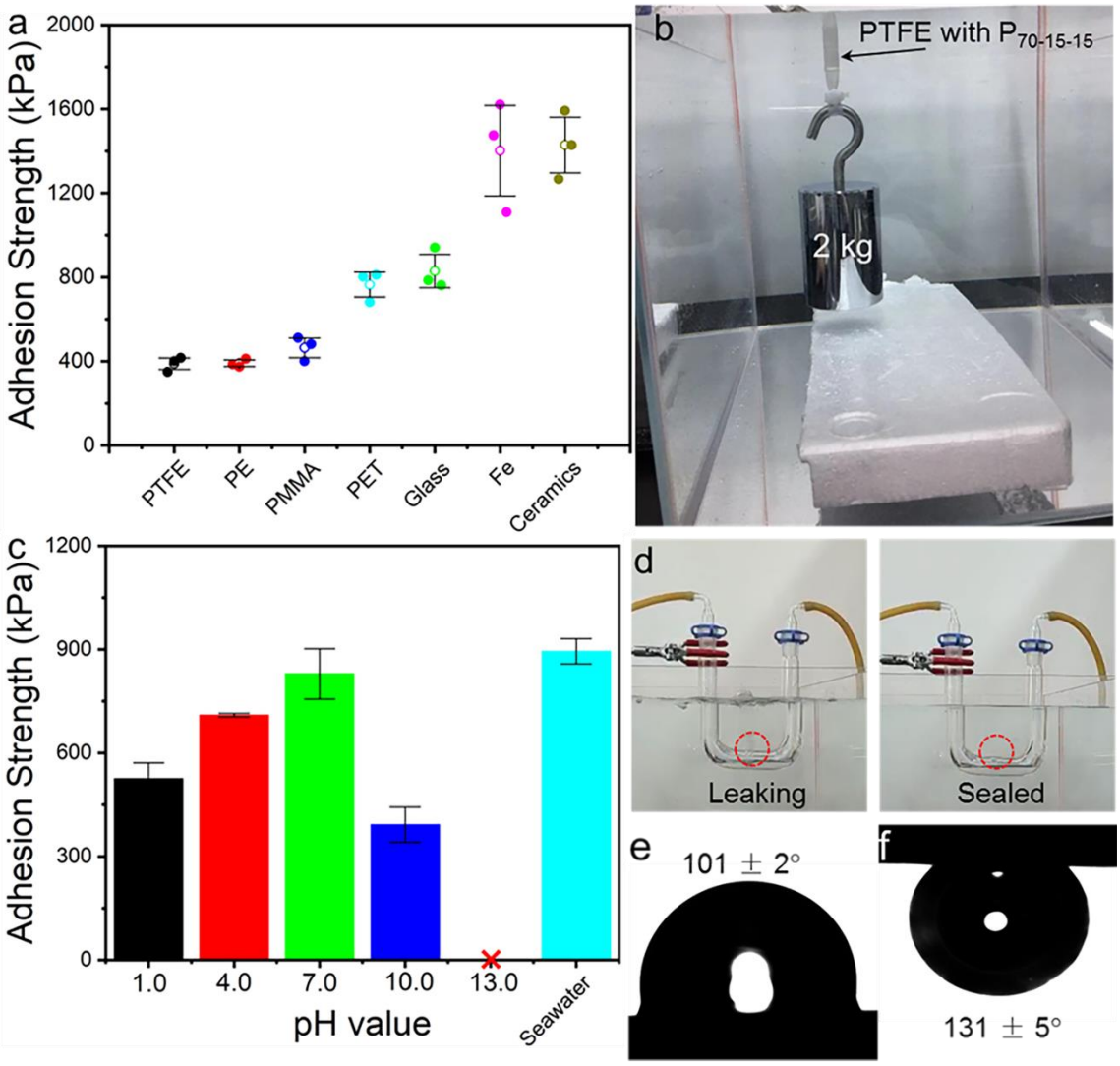

Figure 6. Robust underwater adhesive properties of nucleobase-containing copolymers. (a) Adhesive strengths of $P_{70\text{-}15\text{-}15}$ with distinct substrates including PTFE, PE, PMMA, PET, glass, iron (Fe) and ceramics. (b) A photograph shows that two PTFE films bonded with $P_{70\text{-}15\text{-}15}$ with a contact area of 1.0 cm^2 can hold a weight of 2 kg underwater. (c) Adhesive strengths of $P_{70\text{-}15\text{-}15}$ for glass under seawater and aqueous conditions with different pH values. (d) Photographs showing the underwater leaking gas pipeline can be repaired with $P_{70\text{-}15\text{-}15}$ coated PET film. The exact location of leakage and sealing was marked with a red circle. (e) The contact angle image of seawater and (f) the underwater contact angle image of air bubble on the $P_{70\text{-}15\text{-}15}$ surface show good hydrophobicity in air and underwater aerophobicity.

Underwater spills caused by the rupture of tubes/lines often take place during the extraction and transport of crude oil or natural gas, and such events can give rise to serious environmental issues.[54] Except for the removal of leaked organic pollutants, the immediate

remediation of the leaking point is very important since it can significantly reduce the releasing volume of pollutants. To explore whether our adhesives could find applications in such areas we explored their adhesive tolerance in organic solvents. Interestingly, the complementary H-bonding interactions within $P_{70\text{-}15\text{-}15}$ impart strong adhesive properties in organic solvents such as petroleum ether. The adhesive strength of $P_{70\text{-}15\text{-}15}$ with glass slides is as high as 780 ± 34 kPa in petroleum ether (Figure S27). As shown in Movie S2, we demonstrate that the successful repair of leaking tubes containing petroleum ether (dyed with Sudan II) underwater was achieved instantaneously upon application of a PET film coated with the adhesive $P_{70\text{-}15\text{-}15}$, whereas the control experiment showed that the uncoated PET film is unable to seal the leaking. The underwater contact angle of petroleum ether on the $P_{70\text{-}15\text{-}15}$ coated surface is 113 ± 6°, suggesting an underwater oleophobicity (Figure S27). In contrast, the adhesive failure of $P_{70\text{-}15\text{-}15}$ was observed in CH_2Cl_2 and a $P_{70\text{-}15\text{-}15}$ coated PET film is unable to repair the leak in the tube containing CH_2Cl_2 underwater due to its good wettability on the surface (Figure S27 and Movie S3). Finally, we show that a leaking gas pipeline immersed in seawater can be instantly repaired with PET film coated with the adhesive $P_{70\text{-}15\text{-}15}$ without a long curing time (Figure 6d and Movie S4). The outstanding hydrophobicity in air and underwater aerophobicity of $P_{70\text{-}15\text{-}15}$ render excellent stability to the repaired state (Figure 6e and 6f), which was demonstrated to last for more than 24 h with continuous gas flow.

CONCLUSIONS

In summary, we have developed a new class of instant strong and responsive underwater adhesives through the development of hydrophobic and nucleobase-containing copolymers which are designed to include bioinspired complementary H-bonding interactions.

Furthermore, the high hydrophobicity of the renewable plant oil-based monomer allows for the removal of the interfacial water layer on the adherends without a long curing time. The performance of this new class of hydrophobic nucleobase-containing adhesives substantially outperforms most previously reported underwater hydrogel-based adhesives, with adhesion strength reaching as high as 1.5 MPa and is on a par with that of the strongest underwater adhesives. Additionally, this system also offers fast and excellent responsive adhesive properties with changes in temperature, light, and pH all demonstrating to alter the underwater adhesion properties. These robust supramolecular adhesives have been deployed on various substrates and under a range of different aqueous conditions. As a demonstrator of the potential implementation of these underwater adhesives, we have shown that it was possible to immediately remediate the leaking of oil and gas from an underwater pipe using the adhesives developed here. This work highlights that instant strong and responsive underwater adhesion can be achieved through design of a material with bioinspired supramolecular interactions, enabling many novel applications such as immediate underwater adhesion and repair.

ASSOCIATED CONTENT

Supporting Information.

The Supporting Information is available free of charge.

Synthetic details, ^{1}H NMR spectra, SEC traces of nucleobase-containing copolymers, and underwater adhesive characterization, AFM, rheological analyses, and UV-vis spectra of bioinspired supramolecular polymeric adhesives. (PDF)

AUTHOR INFORMATION

Corresponding Author

*Guangming Liu - Hefei National Laboratory for Physical Sciences at the Microscale, Key Laboratory of Surface and Interface Chemistry and Energy Catalysis of Anhui Higher Education Institutes, Department of Chemical Physics, University of Science and Technology of China, Hefei, Anhui 230026, China; Email: gml@ustc.edu.cn

*Zan Hua - Biomass Molecular Engineering Center and Department of Materials Science and Engineering, Anhui Agricultural University, Hefei, Anhui 230036, China; Email: z.hua@ahau.edu.cn

*Zhongkai Wang - Biomass Molecular Engineering Center and Department of Materials Science and Engineering, Anhui Agricultural University, Hefei, Anhui 230036, China; Email: wangzk6@ahau.edu.cn

Author Contributions

The manuscript was written through contributions of all authors. All authors have given approval to the final version of the manuscript. Z. W., Z. H., and G. L. designed the study. G. Y. and R. K. O. discussed the experiments design. J. W. carried out most of the experiments and analysed the related data. H. L., X. F., B. W. participated in the experiments for monomers and polymers syntheses and adhesive property measurements.

Notes

The authors declare no competing financial interest.

ACKNOWLEDGMENT

This work was financially supported by National Natural Science Foundation of China (22103002, 21873091, 52033001, 51773001, 21622405), Anhui Province Natural Science Funds (2008085QE249), the Fundamental Research Funds for the Central Universities (WK2480000007), and Anhui Provincial Innovation and Entrepreneurship Support Plan for Overseas Returnees (2019LCX023). J. W. also acknowledges the Postgraduate Innovation Fund of Anhui Agricultural University (2021yjs-10) for financial support.

REFERENCES

(1) Li, X., Deng, Y., Lai, J., Zhao, G. and Dong, S. Tough, Long-Term, Water-Resistant, and Underwater Adhesion of Low-Molecular-Weight Supramolecular Adhesives. *J. Am. Chem. Soc.*, **2020**, *142*, 5371-5379.

(2) Cui, C., Fan, C., Wu, Y., Xiao, M., Wu, T., Zhang, D., Chen, X., Liu, B., Xu, Z., Qu, B. and Liu, W. Water‐triggered hyperbranched polymer universal adhesives: from strong underwater adhesion to rapid sealing hemostasis. *Adv. Mater.*, **2019**, *31*, 1905761.

(3) Hong, Y., Zhou, F., Hua, Y., Zhang, X., Ni, C., Pan, D., Zhang, Y., Jiang, D., Yang, L., Lin, Q., Zou, Y., Yu, D., Arnot, D. E., Zou, X., Zhu, L., Zhang, S. and Ouyang, H. A strongly adhesive hemostatic hydrogel for the repair of arterial and heart bleeds. *Nat. Commun.*, **2019**, *10*, 2060.

(4) Sun, J., Xiao, L., Li, B., Zhao, K., Wang, Z., Zhou, Y., Ma, C., Li, J., Zhang, H., Herrmann, A. and Liu, K. Genetically engineered polypeptide adhesive coacervates for surgical applications. *Angew. Chem. Int. Ed.*, **2021**, *60*, 23687-23694.

(5) Yuk, H., Varela, C. E., Nabzdyk, C. S., Mao, X., Padera, R. F., Roche, E. T. and Zhao, X. Dry double-sided tape for adhesion of wet tissues and devices. *Nature*, **2019**, *575*, 169-174.

(6) Deng, J., Yuk, H., Wu, J., Varela, C. E., Chen, X., Roche, E. T., Guo, C. F. and Zhao, X. Electrical bioadhesive interface for bioelectronics. *Nat. Mater.*, **2021**, *20*, 229-236.

(7) Xu, Z., Chen, L., Lu, L., Du, R., Ma, W., Cai, Y., An, X., Wu, H., Luo, Q., Xu, Q., Zhang, Q. and Jia, X. A highly‐adhesive and self‐healing elastomer for bio‐interfacial electrode. *Adv. Funct. Mater.*, **2021**, *31*, 2006432.

(8) Li, J., Celiz, A. D., Yang, J., Yang, Q., Wamala, I., Whyte, W., Seo, B. R., Vasilyev, N. V., Vlassak, J. J., Suo, Z. and Mooney, D. J. Tough adhesives for diverse wet surfaces. *Science*, **2015**, *357*, 378-381.

(9) Rao, P., Sun, T. L., Chen, L., Takahashi, R., Shinohara, G., Guo, H., King, D. R., Kurokawa, T. and Gong, J. P. Tough hydrogels with fast, strong, and reversible underwater adhesion based on a multiscale design. *Adv. Mater.*, **2018**, *30*, 1801884.

(10) Dompé, M., Cedano‐Serrano, F. J., Heckert, O., van den Heuvel, N., van der Gucht, J., Tran, Y., Hourdet, D., Creton, C. and Kamperman, M. Thermoresponsive complex coacervate‐based underwater adhesive. *Adv. Mater.*, **2019**, *31*, 1808179.

(11) Fan, H., Wang, J. and Gong, J. P. Barnacle cement proteins‐inspired tough hydrogels with robust, long‐lasting, and repeatable underwater adhesion. *Adv. Funct. Mater.*, **2021**, *31*, 2009334.

(12) Han, L., Wang, M., Prieto‐López, L. O., Deng, X. and Cui, J. Self‐hydrophobization in a dynamic hydrogel for creating nonspecific repeatable underwater adhesion. *Adv. Funct. Mater.*, **2020**, *30*, 1907064.

(13) Fan, X., Zhou, W., Chen, Y., Yan, L., Fang, Y. and Liu, H. An antifreezing/antiheating hydrogel containing catechol derivative urushiol for strong wet adhesion to various substrates. *ACS Appl. Mater. Inter.*, **2020**, *12*, 32031-32040.

(14) Cui, C., Wu, T., Chen, X., Liu, Y., Li, Y., Xu, Z., Fan, C. and Liu, W. A Janus hydrogel wet adhesive for internal tissue repair and anti‐postoperative adhesion. *Adv. Funct. Mater.*, **2020**, *30*, 2005689.

(15) Qiao, H., Qi, P., Zhang, X., Wang, L., Tan, Y., Luan, Z., Xia, Y., Li, Y. and Sui, K. Multiple weak H-bonds lead to highly sensitive, stretchable, self-adhesive, and self-healing ionic sensors. *ACS Appl. Mater. Inter.*, **2019**, *11*, 7755-7763.

(16) Liu, X., Zhang, Q., Duan, L. and Gao, G. Bioinspired nucleobase-driven nonswellable adhesive and tough gel with excellent underwater adhesion. *ACS Appl. Mater. Inter.*, **2019**, *11*, 6644-6651.

(17) Fan, H., Wang, J., Tao, Z., Huang, J., Rao, P., Kurokawa, T. and Gong, J. P. Adjacent cationic–aromatic sequences yield strong electrostatic adhesion of hydrogels in seawater. *Nat. Commun.*, **2019**, *10*, 5127.

(18) Clancy, S. K., Sodano, A., Cunningham, D. J., Huang, S. S., Zalicki, P. J., Shin, S. and Ahn, B. K. Marine bioinspired underwater contact adhesion. *Biomacromolecules*, **2016**, *17*, 1869-1874.

(19) Beharaj, A., McCaslin, E. Z., Blessing, W. A. and Grinstaff, M. W. Sustainable polycarbonate adhesives for dry and aqueous conditions with thermoresponsive properties. *Nat. Commun.*, **2019**, *10*, 5478.

(20) Wang, Z., Guo, L., Xiao, H., Cong, H. and Wang, S. A reversible underwater glue based on photo- and thermo-responsive dynamic covalent bonds. *Mater. Horiz.*, **2020**, *7*, 282-288.

(21) Liu, X., Zhang, Q., Duan, L. and Gao, G. Tough adhesion of nucleobase-tackifed gels in diverse solvents. *Adv. Funct. Mater.*, **2019**, *29*, 1900450.

(22) Cui, C. and Liu, W. Recent advances in wet adhesives: Adhesion mechanism, design principle and applications. *Prog. Polym. Sci.*, **2021**, *116*, 101388.

(23) Waite, J. H., Andersen, N. H., Jewhurst, S. and Sun, C. Mussel adhesion: finding the tricks worth mimicking. *J. Adhesion*, **2005**, *81*, 297-317.

(24) North, M. A., Del Grosso, C. A. and Wilker, J. J. High strength underwater bonding with polymer mimics of mussel adhesive proteins. *ACS Appl. Mater. Inter.*, **2017**, *9*, 7866-7872.

(25) Chen, X., Yuk, H., Wu, J., Nabzdyk, C. S. and Zhao, X. Instant tough bioadhesive with triggerable benign detachment. *P. Natl. Acad. Sci. USA*, **2019**, *117*, 15497–15503.

(26) Xiao, L., Wang, Z., Sun, Y., Li, B., Wu, B., Ma, C., Petrovskii, V. S., Gu, X., Chen, D., Potemkin, I. I., Herrmann, A., Zhang, H. and Liu, K. An artificial phase-transitional underwater bioglue with robust and switchable adhesion performance. *Angew. Chem. Int. Ed.*, **2021**, *60*, 12082.

(27) Ahn, Y., Jang, Y., Selvapalam, N., Yun, G. and Kim, K. Supramolecular Velcro for Reversible Underwater Adhesion. *Angew. Chem. Int. Ed.*, **2013**, *52*, 3140-3144.

(28) Lutz, J.-F., Thunemann, A. F. and Rurack, K. DNA-like "melting" of adenine- and thymine-functionalized synthetic copolymers. *Macromolecules*, **2005**, *38*, 8124-8126.

(29) Cheng, C.-C., Fan, W.-L., Wu, C.-Y. and Chang, Y.-H. Supramolecular polymer network-mediated structural phase transitions within polymeric micelles in aliphatic alcohols. *ACS Macro Lett.*, **2019**, *8*, 1541-1545.

(30) Huang, C.-W., Ji, W.-Y. and Kuo, S.-W. Water-soluble fluorescent nanoparticles from supramolecular amphiphiles featuring heterocomplementary multiple hydrogen bonding. *Macromolecules*, **2017**, *50*, 7091-7101.

(31) Gebeyehu, B. T., Huang, S.-Y., Lee, A.-W., Chen, J.-K., Lai, J.-Y., Lee, D.-J. and Cheng, C.-C. Dual stimuli-responsive nucleobase-functionalized polymeric systems as efficient tools for manipulating micellar self-assembly behavior. *Macromolecules*, **2018**, *51*, 1189-1197.

(32) Xi, W., Pattanayak, S., Wang, C., Fairbanks, B., Gong, T., Wagner, J., Kloxin, C. J. and Bowman, C. N. Clickable nucleic acids: sequence-controlled periodic copolymer/oligomer synthesis by orthogonal thiol-X reactions. *Angew. Chem. Int. Ed.*, **2015**, *54*, 14462-14467.

(33) Harguindey, A., Domaille, D. W., Fairbanks, B. D., Wagner, J., Bowman, C. N. and Cha, J. N. Synthesis and assembly of click-nucleic-acid-containing PEG-PLGA nanoparticles for DNA delivery. *Adv. Mater.*, **2017**, *29*, 1700743.

(34) Garcia, M., Beecham, M. P., Kempe, K., Haddleton, D. M., Khan, A. and Marsh, A. Water soluble triblock and pentablock poly(methacryloyl nucleosides) from copper-mediated living radical polymerisation using PEG macroinitiators. *Eur. Polym. J.*, **2015**, *66*, 444-451.

(35) Hua, Z., Jones, J. R., Thomas, M., Arno, M. C., Souslov, A., Wilks, T. R. and O'Reilly, R. K. Anisotropic Polymer Nanoparticles with Controlled Dimensions from the Morphological Transformation of Isotropic Seeds. *Nat. Commun.*, **2019**, *10*, 5406.

(36) Hua, Z., Pitto-Barry, A., Kang, Y., Kirby, N., Wilks, T. R. and O'Reilly, R. K. Micellar nanoparticles with tuneable morphologies through interactions between nucleobase-containing synthetic polymers in aqueous solution. *Polym. Chem.*, **2016**, *7*, 4254-4262.

(37) Yan, Y., Gao, C., Li, J., Zhang, T., Yang, G., Wang, Z. and Hua, Z. Modulating morphologies and surface properties of nanoparticles from cellulose-grafted bottlebrush copolymers using complementary hydrogen-bonding between nucleobases. *Biomacromolecules*, **2020**, *21*, 613-620.

(38) Varlas, S., Hua, Z., Jones, J. R., Thomas, M., Foster, J. C. and O'Reilly, R. K. Complementary nucleobase interactions drive the hierarchical self-assembly of core–shell bottlebrush bock copolymers toward cylindrical supramolecules. *Macromolecules*, **2020**, *53*, 9747-9757.

(39) Chen, L., Peng, H., Wei, Y., Wang, X., Jin, Y., Liu, H. and Jiang, Y. Self‐healing properties of PDMS elastomers via guanine and cytosine base pairs. *Macromol. Chem. Phys.*, **2019**, *220*, 1900280.

(40) Liu, X., Zhang, Q. and Gao, G. Bioinspired adhesive hydrogels tackified by nucleobases. *Adv. Funct. Mater.*, **2017**, *27*, 1703132.

(41) Liu, X., Zhang, Q., Gao, Z., Hou, R. and Gao, G. Bioinspired adhesive hydrogel driven by adenine and thymine. *ACS Appl. Mater. Inter.*, **2017**, *9*, 17645-17652.

(42) Cheng, S., Zhang, M., Dixit, N., Moore, R. B. and Long, T. E. Nucleobase self-assembly in supramolecular adhesives. *Macromolecules*, **2012**, *45*, 805-812.

(43) Wu, J., Lei, H., Li, J., Zhang, Z., Zhu, G., Yang, G., Wang, Z. and Hua, Z. Nucleobase-Tackified Renewable Plant Oil-Based Supramolecular Adhesives with Robust Properties Both under Ambient Conditions and Underwater. *Chem. Eng. J.*, **2021**, *405*, 126976.

(44) Ishikawa, N., Furutani, M. and Arimitsu, K. Adhesive materials utilizing a thymine–adenine interaction and thymine photodimerization. *ACS Macro Lett.*, **2015**, *4*, 741-744.

(45) Yuan, L., Wang, Z., Trenor, N. M. and Tang, C. Robust amidation transformation of plant oils into fatty derivatives for sustainable monomers and polymers. *Macromolecules*, **2015**, *48*, 1320-1328.

(46) Song, L., Wang, Z., Lamm, M. E., Yuan, L. and Tang, C. Supramolecular polymer nanocomposites derived from plant oils and cellulose nanocrystals. *Macromolecules*, **2017**, *50*, 7475-7483.

(47) Chang, E. P. Viscoelastic windows of pressure-sensitive adhesives. *J. Adhesion*, **1991**, *34*, 189-200.

(48) Chen, T. T. D., Pena Carrodeguas, L., Sulley, G. S., Gregory, G. L. and Williams, C. K. Bio‐derived and degradable block polyester pressure‐sensitive adhesives. *Angew. Chem. Int. Ed.*, **2020**, *59*, 23450-23455.

(49) Sulley, G. S., Gregory, G. L., Chen, T. T. D., Pena Carrodeguas, L., Trott, G., Santmarti, A., Lee, K. Y., Terrill, N. J. and Williams, C. K. Switchable catalysis improves the properties of CO2-derived polymers: poly(cyclohexene carbonate-b-epsilon-decalactone-b-cyclohexene carbonate) adhesives, elastomers, and toughened plastics. *J. Am. Chem. Soc.*, **2020**, *142*, 4367-4378.

(50) Saito, K., Ingalls, L. R., Lee, J. and Warner, J. C. Core-bound polymeric micellar system based on photocrosslinking of thymine. *Chem. Commun.*, **2007**, *24*, 2503-2505.

(51) Al-Shereiqi, A. S., Boyd, B. J. and Saito, K. Photo-responsive self-assemblies based on bio-inspired DNA-base containing bolaamphiphiles. *Chem. Commun.*, **2015**, *51*, 5460-5462.

(52) Hua, Z., Wilks, T. R., Keogh, R., Herwig, G., Stavros, V. G. and O'Reilly, R. K. Entrapment and rigidification of adenine by a photo-cross-linked thymine network leads to fluorescent polymer nanoparticles. *Chem. Mater.*, **2018**, *30*, 1408-1416.

(53) Zhang, K., Aiba, M., Fahs, G. B., Hudson, A. G., Chiang, W. D., Moore, R. B., Ueda, M. and Long, T. E. Nucleobase-functionalized acrylic ABA triblock copolymers and supramolecular blends. *Polym. Chem.*, **2015**, *6*, 2434-2444.

(54) Flores, J. A., Pavía-Sanders, A., Chen, Y., Pochan, D. J. and Wooley, K. L. Recyclable hybrid inorganic/organic magnetically active networks for the sequestration of crude oil from aqueous environments. *Chem. Mater.*, **2015**, *27*, 3775-3782.